HHS Public Access

Author manuscript

Gastroenterology. Author manuscript; available in PMC 2021 March 01.

Published in final edited form as:

Gastroenterology. 2020 March ; 158(4): 1083–1094. doi:10.1053/j.gastro.2019.11.020.

Mutation That Promotes Activation of Trypsinogen Increases Severity of Secretagogue-Induced Pancreatitis in Mice

Zsanett Jancsó, **Miklós Sahin-Tóth***

Department of Surgery, University of California Los Angeles, Los Angeles, California 90095 and Center for Exocrine Disorders, Department of Molecular and Cell Biology, Boston University Henry M. Goldman School of Dental Medicine, Boston, MA 02118

Abstract

Background & Aims: Mutations in the human serine protease 1 gene (*PRSS1*), which encodes cationic trypsinogen, can accelerate its autoactivation and cause hereditary or sporadic chronic pancreatitis. Disruption of the locus that encodes cationic trypsinogen in mice (T7) causes loss of expression of the protein, but only partially decreases the severity of secretagogue-induced acute pancreatitis and has no effect on chronic pancreatitis. We investigated whether trypsinogen becomes pathogenic only when it is activated by mutation.

Methods: We generated mice with knock-in of the p.K24R mutation (called T7K24R mice), which is analogous to human *PRSS1* mutation p.K23R. We gave T7K24R and C57BL/6N (control) mice repeated injections of cerulein to induce pancreatitis. Plasma amylase activity, pancreatic edema, and myeloperoxidase content in pancreas and lungs and were quantified. We expressed mutant and full-length forms of PRSS1 in *Escherichia coli* and compared their autoactivation.

Results: The p.K24R mutation increased autoactivation of T7 5-fold. T7K24R mice developed no spontaneous pancreatitis. T7K24R mice given cerulein injections had increased pancreatic activation of trypsinogen and edema, infiltration of lung and pancreas by inflammatory cells, and plasma amylase activity compared with control mice given cerulein injections. Injection of cerulein for 2 days induced progressive pancreatitis in T7K24R mice, but not in control mice, with typical features of chronic pancreatitis.

Conclusions: Introduction of a mutation into mice that is analogous to the p.K23R mutation in PRSS1 increases pancreatic activation of trypsinogen during secretagogue-induced pancreatitis. Higher pancreatic activity of trypsin increases the severity of pancreatitis even though loss of trypsin activity does not prevent pancreatitis in mice.

Keywords

genetics; inflammation; mouse model; intrapancreatic

***Correspondence** to Miklós Sahin-Tóth, 675 Charles E Young Drive South, MacDonald Research Laboratories, Rm 2220, Los Angeles, CA 90095. Tel: (310) 267-5905; msahintoth@mednet.ucla.edu.

Author contributions: MST conceived and directed the study. ZJ and MST designed the experiments. ZJ performed the experiments. ZJ and MST analyzed the data. MST wrote the manuscript and ZJ prepared the figures. All authors read and approved the manuscript.

Conflict of interest: No conflicts to declare.

INTRODUCTION

Inflammatory disorders of the human pancreas often form a continuum, which starts with a sentinel attack of acute pancreatitis (AP), followed by recurrent acute attacks (RAP) and eventual development of chronic pancreatitis (CP) [1, 2]. Disease onset and subsequent progression are driven by genetic and environmental factors. The 1996 discovery that mutation p.R122H in human cationic trypsinogen (PRSS1) causes hereditary pancreatitis established the central pathogenic role of trypsin in the AP-RAP-CP sequence [3]. Subsequent human genetic studies not only confirmed but also extended the number of risk factors that promote pancreatitis in a trypsin-dependent manner, both in hereditary and sporadic cases [4]. These susceptibility genes encode digestive proteases or their inhibitor that ultimately determine the extent of premature, intrapancreatic trypsin activation; a key early step in pancreatitis onset. The high impact mutations in the *PRSS1*, *SPINK1* (serine protease inhibitor Kazal type 1) and *CTRC* (chymotrypsin C) genes either promote autoactivation of trypsinogen or reduce the effectiveness of protective trypsin inhibition by SPINK1 or trypsinogen degradation by CTRC [4]. Lower impact genetic changes within the trypsin-dependent pathway are protective and include a haplotype across the *PRSS1-PRSS2* locus that decreases trypsinogen expression; a variant in *PRSS2* (anionic trypsinogen) that results in trypsinogen autodegradation and an inversion at the *CTRB1-CTRB2* locus that alters chymotrypsin B1 and B2 expression causing increased trypsinogen degradation [4]. While genetic studies also uncovered mutations that seem to exert their effect via enzyme misfolding and endoplasmic reticulum stress, the vast majority of clinical cases of pancreatitis is associated with mutations in the trypsin-dependent pathological pathway [5].

Early intrapancreatic trypsin activation is also observed in the secretagogue-hyperstimulation (e.g. cerulein-induced) experimental pancreatitis models in rodents [6–8]. There has been long-standing consensus that trypsin activity is a pathogenic driver in cerulein-induced pancreatitis; however, more recent experiments questioned this belief. Thus, genetic deletion of T7 trypsinogen (T7-KO) abolished intrapancreatic trypsin activation yet only partially protected against AP and had no effect on CP [9, 10]. Curiously, inflammation during AP was unaffected while the extent of acinar cell necrosis was reduced by 50%. Deletion of cathepsin B (*Ctsb*-KO), the main trypsinogen-activating enzyme in this model, resulted in a similar phenotype [10, 11]. On the other hand, mice deficient in protective CTRB1 (*Ctrb1-del* mice) showed elevated intrapancreatic trypsin activation and more severe pancreatitis when given cerulein [12].

Here, we speculated that the contradictory results might be explained by a mechanistic model in which trypsin becomes important as a pathogenic driver only when elevated due to genetic predisposition, while in the genetically unaltered pancreas cerulein-induced trypsin activity plays a lesser role in pancreatitis onset and severity. The new *T7K24R* mouse model described below offers direct proof for this contention.

METHODS

Accession numbers and nomenclature.

NC_000072.6, *Mus musculus* strain C57BL/6J chromosome 6, GRCm38.p4 C57BL/6J; NM_023333.4, *Mus musculus* RIKEN cDNA 2210010C04 gene (2210010C04Rik), mRNA; mouse cationic trypsinogen (isoform T7). Amino-acid residues are numbered starting with the initiator methionine of the primary translation product. Note that because of an extra Asp residue in the activation peptide of T7, amino-acid numbering in this isoform is shifted by one relative to human trypsinogens [13].

Expression plasmids and mutagenesis.

Construction of the pTrapT7-intein-mouse-T7 plasmid was reported previously [14]. During bacterial expression, the intein-trypsinogen fusion undergoes spontaneous self-splicing and T7 trypsinogen with a homogeneous, authentic N terminus is liberated [15]. Mutations were introduced by overlap extension PCR mutagenesis.

Expression and purification of mouse T7 trypsinogen.

Wild-type and mutant intein-trypsinogen fusions were expressed in the aminopeptidase P deficient LG-3 *Escherichia coli* strain [15]. *In vitro* refolding and purification of trypsinogen was performed by ecotin affinity-chromatography [16]. Concentration of trypsinogen was estimated from the UV absorbance at 280 nm using the extinction coefficient 39,140 $M^{-1}cm^{-1}$.

Trypsinogen autoactivation.

Wild-type and p.K24R mutant mouse cationic trypsinogen (isoform T7) was incubated at 2 μM concentration with 10 nM initial trypsin in 0.1 M Tris-HCl (pH 8.0), 1 mM $CaCl_2$ and 0.05% Tween 20 (final concentrations) at 37 °C. At the indicated times, 2 μL aliquots were withdrawn, mixed with 48 μL assay buffer (0.1 M Tris-HCl (pH 8.0), 1 mM $CaCl_2$, 0.05% Tween 20) and trypsin activity was measured by adding 150 μL of 200 μM *N*-CBZ-Gly-Pro-Arg-*p*-nitroanilide substrate (dissolved in assay buffer). Substrate cleavage was measured in a microplate reader at 405 nm wavelength for 1 min and initial rates were plotted.

Trypsinogen activation by cathepsin B and inactivation by cathepsin L.

For the activity assays, cathepsin B (CTSB) purified from human liver was used (catalog number 219362–50UG, EMD Millipore, Temecula, CA). Wild-type and p.K24R mutant mouse cationic trypsinogen (isoform T7) was incubated at 2 μM concentration with 8.5 μg/mL CTSB (~300 nM) at 37 °C in 0.1 M Na-acetate buffer (pH 4.0), 1 mM K-EDTA and 0.05% Tween 20, in 100 μL final volume. The reaction was initiated by adding 2 μL CTSB and at the indicated times 2 μL aliquots were withdrawn and trypsin activity was measured as described under “Trypsinogen autoactivation”.

Activation and inactivation of T7 trypsinogen by cathepsins was also studied by SDS-PAGE using catalytically inactive (p.S201A mutant) T7 constructs. For these experiments we used a recombinant human CTSB preparation [17]. Trypsinogen (1 μM) was incubated at 37 °C in 0.1 M Na-acetate (pH 4.0), and 1 mM K-EDTA with 37 μg/mL human CTSB or 7.1

μg/mL human liver CTSL (219402–25UG, EMD Millipore). Cathepsins were activated with 1 mM dithiothreitol for 20 min before use. Reactions (100 μL) were terminated by precipitation with 10% trichloroacetic acid and analyzed by 15% SDS-PAGE and Coomassie Blue staining.

Animal studies protocol approval.

Animal experiments were performed at Boston University and the University of California Los Angeles (UCLA) with the approval and oversight of the Institutional Animal Care and Use Committee (IACUC) of Boston University and the Animal Research Committee (ARC) at UCLA, including protocol review and post-approval monitoring. The animal care programs at these institutions is managed in full compliance with the US Animal Welfare Act, the United States Department of Agriculture Animal Welfare Regulations, the US Public Health Service Policy on Humane Care and Use of Laboratory Animals and the National Research Council's Guide for the Care and Use of Laboratory Animals. Boston University and UCLA have approved Animal Welfare Assurance statements (A3316–01 and A3196–01, respectively) on file with the US Public Health Service, National Institutes of Health, Office of Laboratory Animal Welfare. Both institutions are accredited by the Association for Assessment and Accreditation of Laboratory Animal Care International (AAALAC).

Generation of the *T7K24R* mouse strain.

Mice were on the C57BL/6N genetic background. The gene encoding T7 trypsinogen (2210010C04Rik) is located on chromosome 6; it spans ~3.8 kb and comprises 5 exons. Mutation c.71A>G (p.K24R) was knocked-in using homologous recombination in C57BL/6 embryonic stem (ES) cells (Cyagen, Santa Clara, CA). The targeting vector contained the T7 trypsinogen gene with the p.K24R mutation in exon 2 and a 1,922 nt sequence including a neomycin resistance gene flanked by loxP sites in intron 1 (Supplementary Figure 1). Correctly targeted ES cell clones were identified by long-range PCR and confirmed by Southern blot. Mutant ES cells were injected into mouse embryos (blastocysts), which were implanted into pseudopregnant females. The resulting chimeras were bred with wild-type C57BL/6N mice to achieve germline transmission of the mutant allele. To remove the neomycin resistance gene from the mutant allele, mice were bred with a Cre-deleter strain that expresses the Cre recombinase in the early mouse embryo (B6.FVB-Tg(EIIa-cre)C5379Lmgd/J; Jackson Laboratories). The final *T7K24R* knock-in allele contained the p.K24R mutation in exon 2 and a 125 nt residual sequence in intron 1 including a single loxP site (Supplementary Figure 2). *T7K24R* mice were maintained in the homozygous state. C57BL/6N mice obtained from Charles River Laboratories (Wilmington, MA) or produced in our breeding facility from the same stock were used as experimental controls. The number of animals used in each experiment is shown in the figures. Both male and female animals were studied. Experimental mice were 11–12 weeks old and weighed around 25 g (males) and 20 g (females).

Genotyping.

To genotype *T7K24R* mice, we used primers that amplified exon 2 with the flanking intronic sequences. The amplicon size from the wild-type allele was 630 bp, whereas the mutant

allele yielded a 755 bp product due to the presence of the residual sequence in intron 1. The primer sequences were as follows. Forward primer, 5'- CTT GAA ACT AAC AGT GGA CCC T −3'; reverse primer, 5'- AAC TGT GCA CAT TTC CTA ATT G −3'.

Quantitative reverse transcription (RT)-PCR.

Expression levels of T7 trypsinogen mRNA were determined by RT-PCR. Total RNA was extracted from mouse pancreas (~30 mg tissue) using the RNeasy Plus Mini Kit (catalog number 74136, Qiagen, Valencia, CA). RNA (2 μg) was reverse-transcribed using the High Capacity cDNA Reverse Transcription Kit (catalog number 4368814, Thermo Fisher Scientific). Real-time PCR was performed with the iTaq Universal SYBR Green Supermix (catalog number 1725121, Bio-Rad Laboratories, Inc.), using the following primers. Forward primer, 5'– ACC TTA ATC TTC CTT GCC TTC −3'; reverse primer, 5'– CCA CTG GGA ATT GAT GAG TGA −3'. These primers amplify a 168 nt region between c.7 and c.174 of the T7 trypsinogen coding sequence. A 252 nt region of the 18S ribosomal RNA was amplified as the housekeeping gene control using forward primer 5'- GAA ACG GCT ACC ACA TCC AAG G −3' and reverse primer 5'- CCG CTC CCA AGA TCC AAC TAC G −3'. Relative expression levels were estimated with the comparative cycle threshold method (ΔΔCT method). First, CT values for T7 trypsinogen were normalized to those of the 18S rRNA reference gene (ΔCT) and then to the ΔCT value of the C57BL/6N sample (ΔΔCT). Results were expressed as fold change calculated with the formula 2−ΔΔCT.

Western blotting.

Immunoblotting was performed as described in [14]. T7 trypsinogen was detected using a rabbit polyclonal antibody raised against the peptide sequence LKTAATLNSRVST corresponding to amino-acids 114–126 of mouse T7 pre-trypsinogen [14]. The specificity of the antibody was previously validated on pancreas homogenate from T7-deficient mice. The antibody was used at a final dilution of 1:10,000. Mouse SPINK3 was detected with a rabbit polyclonal antibody used at a dilution of 1:1,000 (catalog number 2744, Cell Signaling Technology). Rabbit monoclonal antibody against p44/42 MAPK (ERK1/2) (137F5) was used at a final dilution of 1:1,000 (catalog number 4695, Cell Signaling Technology). The horse-radish peroxidase-conjugated goat anti-rabbit secondary antibody was used at a dilution of 1:10,000 (catalog number 31460, Thermo Fisher Scientific).

Cerulein-induced pancreatitis.

Acute pancreatitis was induced by repeated intraperitoneal injections of the secretagogue peptide cerulein in a supramaximal stimulatory dose. Cerulein (catalog number C9026, Sigma-Aldrich, St. Louis, MO) was dissolved in normal saline and injected hourly 12 times at a dose of 50 μg/kg. Experimental controls received normal saline injections. Mice were sacrificed 1 h after the last injection and the pancreas, lung tissue and blood were harvested. For histological analysis, pancreas tissue was fixed in 10% neutral buffered formalin. For myeloperoxidase (MPO) assays, pancreas and lung tissue was flash frozen in liquid nitrogen and stored at −80°C until use. Blood was collected in heparinized syringes; cells were removed by centrifugation at 2,000g for 15 min at 4°C and the plasma was stored frozen at −80°C until use.

For sustained stimulation with cerulein, hourly injections were performed 8 times per day on two consecutive days. Controls were given normal saline injections. Mice were sacrificed 3 days and 10 days after the last injection.

Determination of pancreatic water content.

To characterize tissue edema, a 50–100 mg portion of the pancreas was weighed, dried for 72 hours in an oven at 65°C and weighed again. Tissue water content was then expressed as percent of wet mass.

Plasma amylase.

Levels of amylase in blood plasma were determined using the 2-chloro-*p*-nitrophenyl-α-D-maltotrioside substrate (catalog number A7564–60, Pointe Scientific, Canton, MI). Plasma (0.5 μL) was diluted with 9 μL normal saline and mixed with 190 μL substrate to start the reaction. The increase in absorbance due to the release of 2-chloro-nitrophenol was followed at 405 nm for 2 min. Rate of substrate cleavage was expressed in mOD/min units.

Pancreas and lung myeloperoxidase (MPO) content.

To evaluate inflammatory cell infiltration, MPO content of the tissue was determined using an ELISA kit (catalog number HK210–01, Hycult Biotech, Plymouth Meeting, PA) according to the manufacturer's instructions. The ELISA signal measured at 450 nm was converted to ng/mL MPO concentration using a calibration curve; normalized to total protein concentration and expressed as ng MPO/mg protein.

Histology and immunohistochemistry.

Pancreas tissue was fixed in 10% neutral buffered formalin; paraffin-embedded (FFPE); sectioned and stained with hematoxylin-eosin or Masson's trichrome staining, as indicated, at the Boston University Experimental Pathology Laboratory Service Core. Arbitrary scoring (scale 0–3) by visual inspection was used to semi-quantitate the extent of tissue edema and inflammatory cell infiltration. 0 = absent, 1 = minimal (<10% of visual field), 2 = moderate (10% to 50%), and 3 = severe (>50%). Acinar cell necrosis was estimated by visual inspection and expressed as percent of tissue area. Staining for the leukocyte markers MPO, F4/80, CD3, CD45R/B220 and the apoptosis marker active/cleaved caspase 3 was carried out at the Specialized Histopathology Core, Brigham and Women's Hospital, Boston, MA and at the Translational Pathology Core Laboratory of UCLA, as described previously [14].

Intrapancreatic trypsin and chymotrypsin activation.

Cerulein-induced intrapancreatic protease activation was determined at 30 min after a single cerulein (50 μg/kg) injection. The pancreas (~40 mg) was homogenized in 1 mL MOPS homogenization buffer (250 mM sucrose, 5 mM MOPS (pH 6.5), 1 mM $MgSO_4$), using a rotor-stator homogenizer (Tissue Master 125, Omni International, Kennesaw, GA). The homogenate was briefly centrifuged (1,000 g, 2 min, 4°C), and trypsin and chymotrypsin activity in the supernatant was determined using the Z-Gly-Pro-Arg-AMC·HCl and Suc-Ala-Ala-Pro-Phe-AMC fluorescent substrates (Bachem USA, Torrance, CA), respectively. Aliquots (5 μL) of the cleared homogenate were mixed with 45 μL assay buffer (0.1 M Tris-

HCl (pH 8.0), 1 mM $CaCl_2$, 0.05% Tween 20) and 150 μL of 200 μM substrate dissolved in assay buffer was added to initiate the reaction. The increase in fluorescence was followed for 5 min in a fluorescent plate reader at 380 nm excitation and 460 nm emission wavelengths. The rate of substrate cleavage was expressed as relative fluorescent units (RFU) per second and it was normalized to the total protein in the assay mix (RFU/sec/mg protein).

Propidium iodide uptake in isolated pancreatic acinar cells.

Pancreatic acinar cells were isolated by collagenase digestion as described in the Supplementary Methods. Acinar cells (0.5 mL per well) were treated with 100 nM cerulein or the same volume of normal saline for 3 hours and then 1 μL propidium iodide (PI, 1 mg/mL aqueous solution, catalog number J66584, Thermo Fisher Scientific) was added. After 10 min incubation, the cells were pelleted in an eppendorf tube by a quick centrifugation and the supernatant containing the excess PI was removed. The cells were washed with phosphate-buffered saline and resuspended in 250 μL lysis buffer containing 50 mM Tris-HCl (pH 7.4), 150 mM NaCl, 1% Triton X-100 and 0.1% SDS supplemented with Halt protease and phosphatase inhibitor cocktail (100x solution, catalog number 1861284, Thermo Fisher Scientific). Debris was pelleted by brief centrifugation and the PI fluorescence was measured from the supernatant at 535 nm excitation and 617 nm emission wavelengths. The fluorescence readings were normalized to the total protein content. Results were expressed as fold increase in fluorescence relative to control acinar cells given normal saline.

Statistical analysis.

Results were plotted as individual data points with the mean and standard deviation indicated. Differences of means between two groups were analyzed by unpaired t-test. $P < 0.05$ was considered statistically significant.

RESULTS

Effect of the p.K24R mutation on T7 trypsinogen.

We hypothesized that increased intrapancreatic activation of mouse T7 trypsinogen will worsen cerulein-induced pancreatitis. To test this notion, we introduced the human hereditary-pancreatitis-associated mutation p.K23R into the activation peptide of mouse T7 trypsinogen, in which the corresponding mutation is p.K24R (Figure 1A). The p.K23R mutation is a relatively rare human variant, which has been found in 12 CP patients worldwide but never in healthy controls [18–21]. Biochemical studies indicated that the mutation increases autoactivation of human cationic trypsinogen at least 5-fold [22, 23]. The mutation changes the activation site Lys to an Arg, which is a better substrate for trypsin, resulting in accelerated trypsin-mediated trypsinogen activation, i.e. autoactivation. To ascertain that the p.K24R mutation has the same stimulatory effect on mouse T7 trypsinogen, we expressed wild-type and mutant T7 trypsinogen recombinantly and compared autoactivation of purified trypsinogen preparations (Figure 1B). We found that the p.K24R mutant autoactivated about 5-fold faster than wild-type T7 trypsinogen. Intrapancreatic activation of T7 trypsinogen can also be mediated by cathepsin B (CTSB), while cathepsin L (CTSL) can inactivate T7 trypsinogen by cleaving after Gly27 [24].

Importantly, mutation p.K24R did not increase CTSB-mediated activation or alter CTSL-mediated inactivation of T7 trypsinogen, indicating that the effect of the mutation is specific for autoactivation (Figure 1C, Supplementary Figure 3).

Generation of the *T7K24R* knock-in mouse model.

We knocked-in the p.K24R mutation to the endogenous mouse T7 trypsinogen gene locus using homologous recombination in the C57BL/6N genetic background (Supplementary Figure 4A). The correctly targeted allele contained mutation p.K24R in exon 2 and a neomycin resistance gene flanked by two loxP sites in the neighboring intron 1 (Supplementary Figure 1). To remove the neomycin cassette, mice were bred with a Cre deleter strain, which expresses the Cre recombinase in the mouse embryo. The final *T7K24R* mutant strain contained the p.K24R mutation in exon 2 and a 125 nt scar sequence including a single loxP site in intron 1 of the T7 trypsinogen gene (Supplementary Figure 2). Although pancreatitis-associated human cationic trypsinogen mutations are heterozygous, we bred the *T7K24R* mice to homozygosity to obtain more pronounced effects. Relative to the C57BL/6N parent strain, expression of mutant T7 trypsinogen was comparable both at the mRNA (Supplementary Figure 4B) and protein levels (Supplementary Figure 4C). Expression of the trypsin inhibitor protein SPINK3 was not upregulated in the pancreas of *T7K24R* mice, as judged by western blot analysis (Supplementary Figure 4D). Homozygous *T7K24R* mice developed and bred normally and showed no obvious phenotypic alterations. Pancreas histology was also normal up to one year of age. In one-year-old *T7K24R* mice, we occasionally observed patchy acinar cell damage and focal cellular infiltrates adjacent to slightly distorted islets (Supplementary Figure 5).

Cerulein-induced acute pancreatitis in *T7K24R* mice.

We induced pancreatitis in *T7K24R* and C57BL/6N mice with 12 hourly injections of the secretagogue cerulein used at a supramaximal stimulatory dose (50 μg/kg). Control mice received normal saline injections. We characterized pancreatitis responses by measuring pancreatic edema, plasma amylase activity, pancreas myeloperoxidase (MPO) content and by histological evaluation of hematoxylin-eosin stained pancreas sections. When mice were sacrificed one hour after the last injection, we observed a white, enlarged pancreas in cerulein-treated C57BL/6N mice, indicating pancreas edema (Figure 2A). Remarkably, *T7K24R* mice exhibited a markedly engorged pancreas with visible lobule boundaries (Figure 2A). Measurement of pancreas mass (Figure 2B) and pancreatic water content (Figure 2C) corroborated the prominent edema in *T7K24R* mice. Plasma amylase activity (Figure 3A) and pancreas MPO content (Figure 3B) were also significantly increased in cerulein-treated *T7K24R* mice relative to C57BL/6N mice. Finally, measurement of lung MPO content indicated that systemic inflammation was significantly higher in *T7K24R* mice versus C57BL/6N mice (Figure 3C). Thus, mutation p.K24R in T7 trypsinogen increased all investigated parameters of acute pancreatitis elicited by cerulein injections.

Histological evaluation and scoring of pancreas tissue confirmed the biochemical results; massive edema and inflammatory cell infiltration was evident in cerulein-injected *T7K24R* mice when compared to similarly treated C57BL/6N mice, which exhibited less pronounced changes (Figure 4). Under the experimental conditions employed, the C57BL/6N strain

developed little necrosis (~3%) in response to cerulein injections, and a trend for increased necrosis (~4%) was observed in *T7K24R* mice, which did not reach statistical significance (Figure 4B). We evaluated pancreas sections for active/cleaved caspase 3 as a marker of apoptosis with immunohistochemistry and saw scattered staining in both strains with a slightly higher number of positive cells in the *T7K24R* sample (Supplementary Figure 6). Finally, we used immunohistochemistry to analyze the inflammatory cell infiltrate in cerulein-treated *T7K24R* mice. Pancreas sections were strongly positive for MPO and F4/80, indicating that the cells represent neutrophil granulocytes and macrophages. In contrast, no staining was obtained for the T and B lymphocyte markers CD3 and CD45R/B220, respectively (Supplementary Figure 7).

Cerulein-induced injury in isolated acinar cells.

We were surprised to find that acinar cell necrosis was not elevated significantly in *T7K24R* mice given cerulein versus similarly treated C57BL6/N mice. To investigate this further, we incubated isolated pancreatic acinar cells with 100 nM cerulein and measured propidium iodide uptake as a marker of cell injury. No significant differences were observed between acinar cell preparations from *T7K24R* and C57BL/6N mice (Supplementary Figure 8).

Cerulein-induced chronic pancreatitis in *T7K24R* mice.

To assess whether sustained challenge with repeated cerulein injections would result in more pronounced cellular injury in *T7K24R* mice, we performed a 2-day cerulein injection model, with 8 hourly injections on two consecutive days (Figures 5 and 6). Mice were sacrificed at 3 days and 10 days after the last injection. We evaluated the effects of the extended cerulein treatment by measuring pancreas mass and by histological analysis of pancreas sections stained with hematoxylin-eosin or Masson's trichrome staining. At 3 days after cerulein treatment, the pancreas of C57BL/6N mice showed only minimal changes whereas essentially complete acinar cell ablation was observed in the pancreas of *T7K24R* mice. Acinar cell dropout was accompanied by the appearance of tubular complexes, inflammatory cell infiltrates and diffuse fibrosis. The pancreas mass of *T7K24R* mice was significantly reduced relative to C57BL/6N mice, consistent with acinar cell atrophy. At 10 days, histology of the pancreas from C57BL/6N mice looked normal, whereas the pancreas of *T7K24R* mice showed some recovery of acinar tissue and classic hallmarks of chronic pancreatitis including acinar cell loss, strong fibrosis, dilated ducts and tubular complexes. Notably, pancreas mass in *T7K24* mice was markedly reduced (Figure 6). Thus, it appears that prolonged challenge with cerulein induces severe and progressive pancreatitis in *T7K24R* mice with chronic pancreatitis-like pathology.

Intrapancreatic trypsin activation in *T7K24R* mice.

To demonstrate that the heightened pancreatitis responses in *T7K24R* mice given cerulein were caused by increased intrapancreatic trypsin activation, we measured trypsin activity from pancreas homogenates of mice. For these experiments, we injected mice with cerulein once and then sacrificed them 30 min later. This is the optimal time point to assess trypsin activation in mice [9]. Furthermore, under these conditions, we can avoid the confounding effects of inflammatory cell infiltrates and acinar cell damage that occur during the course of the acute pancreatitis elicited by repeated cerulein injections. Cerulein induced

intrapancreatic trypsin activation in both *T7K24R* and C57BL/6N mice (Figure 7A). However, trypsin levels were significantly higher in *T7K24R* mice, consistent with the increased propensity for autoactivation of the p.K24R mutant trypsinogen. In contrast, intrapancreatic chymotrypsin activation was comparable in *T7K24R* and C57BL/6N mice, suggesting that maximal activation was achieved with either trypsin levels (Figure 7B).

DISCUSSION

Here we present the novel *T7K24R* mouse model harboring a human hereditary-pancreatitis associated mutation in the native mouse cationic trypsinogen (isoform T7), which increases autoactivation of trypsinogen to trypsin. Consequently, when trypsinogen activation is initiated inside acinar cells by pathological stimuli such as cerulein hyperstimulation, *T7K24R* mice respond with higher trypsin activation. Remarkably, elevated trypsin activity in the *T7K24R* mice is associated with heightened pancreatitis responses elicited by repeated cerulein injections. Thus, plasma amylase activity, pancreas edema and inflammatory cell infiltration of the pancreas and the lungs were all markedly elevated in *T7K24R* mice relative to C57BL/6N mice. All parameters of acute pancreatitis worsened indicating that trypsin likely acts as an initiating factor for the disease. Sustained challenge with cerulein for 2 days resulted in progressive pancreatitis in the *T7K24R* mice with characteristic features of chronic pancreatitis, including marked atrophy and widespread fibrosis. The observations convey a simple message: more trypsin equals more pancreatitis.

A somewhat puzzling aspect of our findings is that pancreatic acinar cell necrosis seemed to be comparable in C57BL/6N and *T7K24R* mice given cerulein. Experiments with isolated acinar cells confirmed that cerulein induced a similar extent of injury in the two mouse strains. These observations are counterintuitive and argue that increased pancreatitis severity in the *T7K24R* mice is not driven by more extensive acinar cell necrosis. One can speculate that trypsin might exert some of its proinflammatory effects extracellularly, possibly through proteinase-activated receptors.

Our findings with the *T7K24R* mice are fully consistent with the proposed central role of trypsin in human pancreatitis, which was based on genetic studies coupled with biochemical and cell biological investigations of the mutational effects [4]. As described in the introduction, the trypsin-dependent pathological pathway seems to underlie a large fraction of human cases that exhibit the AP>RAP>CP disease progression and are commonly referred to as CP. Despite the solid evidence in human CP, the pathogenic role of trypsin was recently questioned based on the properties of the T7 trypsinogen deleted (T7-KO) mice [9, 10]. T7-KO mice exhibited diminished intrapancreatic trypsin activation when given cerulein yet their AP responses were essentially unchanged with the exception of a 50% decrease in acinar cell necrosis [9]. In a cerulein-induced CP model, none of the severity parameters showed an appreciable difference between T7-KO and control mice [10]. The phenotype of T7-KO mice with respect to cerulein-induced pancreatitis is similar to that of CTSB-deficient mice, which do not exhibit intrapancreatic trypsin activation yet their pathological responses are only partially mitigated in AP and are unaltered in CP [10, 11]. Thus, abolishing intrapancreatic trypsin activation either by deletion of T7 trypsinogen or by genetic disruption of CTSB in mice has a limited impact on AP and no effect on CP.

To reconcile these earlier observations with the present data, we propose that in the absence of any genetic changes, the role of trypsin in cerulein-induced pancreatitis is limited and pancreatitis responses are primarily driven by other signaling pathways triggered by cerulein [25]. This notion is consistent with studies showing that trypsin is responsible for increased organellar fragility but not the other cellular events that characterize pancreatitis onset [26]. A different situation emerges when trypsinogen is mutated or when mechanisms responsible for trypsin inhibition or degradation are genetically compromised. Under these conditions, intrapancreatic trypsin activation becomes significantly elevated and the higher trypsin levels now become the pathogenic driver for the disease. This manifests as more severe pancreatitis in the cerulein model in mice and in the development of the AP-RAP-CP disease sequence in humans. It is notable that the phenotype of the recently published *Ctrb1-del* mice in which protective CTRB1 was deleted is remarkably similar to that of the *T7K24R* mice both in terms of increased intrapancreatic trypsin activation and the more severe pancreatitis responses [12]. This lends credence to our hypothesis that trypsin-dependent pancreatitis primarily occurs in the setting of appropriate genetic changes that cause increased trypsin activation.

The pathogenic role of excessive trypsin activity is clearly supported by other mouse models such as transgenic mice carrying a furin-activated rat trypsinogen construct [27, 28], transgenic mice with the human *PRSS1* gene containing the p.R122H mutation [29, 30] or the *T7D23A* mouse model, which contains the p.D23A mutation in the activation peptide of T7 trypsinogen [14]. Mutation p.D23A increases trypsinogen autoactivation 50-fold and heterozygous mice develop spontaneous, early-onset AP that rapidly progresses to CP. The *T7K24R* model described in this paper does not develop spontaneous disease, because the stimulating effect of the p.K24R mutation on autoactivation is smaller (5-fold) and pancreatic defense mechanisms can efficiently cope with the higher propensity for trypsin activation. Both the *T7D23A* and *T7K24R* mouse strains represent important preclinical models useful for testing of novel therapeutics. *T7D23A* mice are attractive because they develop spontaneous disease driven by trypsin, which mimics the course of human hereditary pancreatitis the best. However, age of onset is variable, which makes experimental design and interpretation difficult. On the other hand, trypsin-dependent pancreatitis can be readily studied in *T7K24R* mice in a more controlled manner, where disease-onset can be initiated synchronously and pancreatitis responses can be measured at well-defined time points. The availability of these two remarkable mouse models should finally open up avenues for therapeutic targeting of trypsin to prevent and treat pancreatitis.

Supplementary Material

Refer to Web version on PubMed Central for supplementary material.

Acknowledgements:

This work was supported by the Department of Defense grant W81XWH-14-1-0331, National Institutes of Health (NIH) grants R01 DK117809, R01 DK058088 and R01 DK082412 (to MST), and a grant from the National Pancreas Foundation (to ZJ).

Abbreviations:

AP	acute pancreatitis
CP	chronic pancreatitis
CTRB1	chymotrypsin B1
CTRB2	chymotrypsin B2
CTRC	chymotrypsin C
CTSB	cathepsin B
CTSL	cathepsin L
MPO	myeloperoxidase
PRSS1	serine protease 1, human cationic trypsinogen
PRSS2	serine protease 2, human anionic trypsinogen
RAP	recurrent acute pancreatitis
RT-PCR	reverse transcription polymerase chain reaction
SPINK1	serine protease inhibitor Kazal type 1
SPINK3	mouse ortholog of human SPINK1
T7	mouse cationic trypsinogen
T7K24R	mouse cationic trypsinogen allele with p.K24R mutation

REFERENCES

1. Yadav D, Lowenfels AB. The epidemiology of pancreatitis and pancreatic cancer. Gastroenterology 2013, 144:1252–1261 [PubMed: 23622135]
2. Whitcomb DC, Frulloni L, Garg P, Greer JB, Schneider A, Yadav D, Shimosegawa T. Chronic pancreatitis: An international draft consensus proposal for a new mechanistic definition. Pancreatology 2016, 16:218–224 [PubMed: 26924663]
3. Whitcomb DC, Gorry MC, Preston RA, Furey W, Sossenheimer MJ, Ulrich CD, Martin SP, Gates LK Jr, Amann ST, Toskes PP, Liddle R, McGrath K, Uomo G, Post JC, Ehrlich GD. Hereditary pancreatitis is caused by a mutation in the cationic trypsinogen gene. Nat Genet 1996, 14:141–145 [PubMed: 8841182]
4. Hegyi E, Sahin-Tóth M. Genetic risk in chronic pancreatitis: The trypsin-dependent pathway. Dig Dis Sci 2017, 62:1692–1701 [PubMed: 28536777]
5. Sahin-Tóth M Genetic risk in chronic pancreatitis: the misfolding-dependent pathway. Curr Opin Gastroenterol 2017, 33:390–395 [PubMed: 28650851]
6. Hofbauer B, Saluja AK, Lerch MM, Bhagat L, Bhatia M, Lee HS, Frossard JL, Adler G, Steer ML. Intra-acinar cell activation of trypsinogen during caerulein-induced pancreatitis in rats. Am J Physiol 1998, 275:G352–362 [PubMed: 9688663]
7. Lerch MM, Gorelick FS. Early trypsinogen activation in acute pancreatitis. Med Clin North Am 2000, 84:549–563 [PubMed: 10872413]

8. Saluja AK, Lerch MM, Phillips PA, Dudeja V. Why does pancreatic overstimulation cause pancreatitis? Annu Rev Physiol 2007, 69:249–269 [PubMed: 17059357]
9. Dawra R, Sah RP, Dudeja V, Rishi L, Talukdar R, Garg P, Saluja AK. Intra-acinar trypsinogen activation mediates early stages of pancreatic injury but not inflammation in mice with acute pancreatitis. Gastroenterology 2011, 141:2210–2217 [PubMed: 21875495]
10. Sah RP, Dudeja V, Dawra RK, Saluja AK. Cerulein-induced chronic pancreatitis does not require intra-acinar activation of trypsinogen in mice. Gastroenterology 2013, 144:1076–1085 [PubMed: 23354015]
11. Halangk W, Lerch MM, Brandt-Nedelev B, Roth W, Ruthenbuerger M, Reinheckel T, Domschke W, Lippert H, Peters C, Deussing J. Role of cathepsin B in intracellular trypsinogen activation and the onset of acute pancreatitis. J Clin Invest 2000, 106:773–781 [PubMed: 10995788]
12. Jancsó Z, Hegyi E, Sahin-Tóth M. Chymotrypsin reduces the severity of secretagogue-induced pancreatitis in mice. Gastroenterology 2018, 155:1017–1021 [PubMed: 30076839]
13. Németh BC, Wartmann T, Halangk W, Sahin-Tóth M. Autoactivation of mouse trypsinogens is regulated by chymotrypsin C via cleavage of the autolysis loop. J Biol Chem 2013, 288:24049–24062 [PubMed: 23814066]
14. Geisz A, Sahin-Tóth M. A preclinical model of chronic pancreatitis driven by trypsinogen autoactivation. Nat Commun 2018, 9:5033 [PubMed: 30487519]
15. Király O, Guan L, Szepessy E, Tóth M, Kukor Z, Sahin-Tóth M. Expression of human cationic trypsinogen with an authentic N terminus using intein-mediated splicing in aminopeptidase P deficient Escherichia coli. Protein Expr Purif 2006, 48:104–111 [PubMed: 16542853]
16. Király O, Guan L, Sahin-Tóth M. Expression of recombinant proteins with uniform N-termini. Methods Mol Biol 2011, 705:175–194 [PubMed: 21125386]
17. Steed PM, Lasala D, Liebman J, Wigg A, Clark K, Knap AK. Characterization of recombinant human cathepsin B expressed at high levels in baculovirus. Protein Sci 1998, 7:2033–2037. [PubMed: 9761485]
18. Férec C, Raguénès O, Salomon R, Roche C, Bernard JP, Guillot M, Quéré I, Faure C, Mercier B, Audrézet MP, Guillausseau PJ, Dupont C, Munnich A, Bignon JD, Le Bodic L. Mutations in the cationic trypsinogen gene and evidence for genetic heterogeneity in hereditary pancreatitis. J Med Genet 1999, 36:228–232 [PubMed: 10204851]
19. Werlin S, Konikoff FM, Halpern Z, Barkay O, Yerushalmi B, Broide E, Santo E, Shamir R, Shaoul R, Shteyer E, Yaakov Y, Cohen M, Kerem E, Ruszniewski P, Masson E, Ferec C, Wilschanski M. Genetic and electrophysiological characteristics of recurrent acute pancreatitis. J Pediatr Gastroenterol 2015, 60:675–679
20. Giefer MJ, Lowe ME, Werlin SL, Zimmerman B, Wilschanski M, Troendle D, Schwarzenberg SJ, Pohl JF, Palermo J, Ooi CY, Morinville VD, Lin TK, Husain SZ, Himes R, Heyman MB, Gonska T, Gariepy CE, Freedman SD, Fishman DS, Bellin MD, Barth B, Abu-El-Haija M, Uc A. Early-onset acute recurrent and chronic pancreatitis is associated with PRSS1 or CTRC gene mutations. J Pediatr 2017, 186:95–100 [PubMed: 28502372]
21. Jalaly NY, Moran RA, Fargahi F, Khashab MA, Kamal A, Lennon AM, Walsh C, Makary MA, Whitcomb DC, Yadav D, Cebotaru L, Singh VK. An evaluation of factors associated with pathogenic PRSS1, SPINK1, CTFR, and/or CTRC genetic variants in patients with idiopathic pancreatitis. Am J Gastroenterol 2017, 112:1320–1329 [PubMed: 28440306]
22. Chen JM, Kukor Z, Le Maréchal C, Tóth M, Tsakiris L, Raguénès O, Férec C, Sahin-Tóth M. Evolution of trypsinogen activation peptides. Mol Biol Evol 2003, 20:1767–1777 [PubMed: 12832630]
23. Geisz A, Hegyi P, Sahin-Tóth M. Robust autoactivation, chymotrypsin C independence and diminished secretion define a subset of hereditary pancreatitis-associated cationic trypsinogen mutants. FEBS J 2013, 280:2888–2899 [PubMed: 23601753]
24. Wartmann T, Mayerle J, Kähne T, Sahin-Tóth M, Ruthenbürger M, Matthias R, Kruse A, Reinheckel T, Peters C, Weiss FU, Sendler M, Lippert H, Schulz HU, Aghdassi A, Dummer A, Teller S, Halangk W, Lerch MM. Cathepsin L inactivates human trypsinogen, whereas cathepsin L-deletion reduces the severity of pancreatitis in mice. Gastroenterology 2010, 138:726–737 [PubMed: 19900452]

25. Williams JA. Cholecystokinin (CCK) regulation of pancreatic acinar cells: Physiological actions and signal transduction mechanisms. Compr Physiol 2019, 9:535–564 [PubMed: 30873601]

26. Van Acker GJ, Weiss E, Steer ML, Perides G. Cause-effect relationships between zymogen activation and other early events in secretagogue-induced acute pancreatitis. Am J Physiol Gastrointest Liver Physiol 2007, 292:G1738–1746 [PubMed: 17332471]

27. Gaiser S, Daniluk J, Liu Y, Tsou L, Chu J, Lee W, Longnecker DS, Logsdon CD, Ji B. Intracellular activation of trypsinogen in transgenic mice induces acute but not chronic pancreatitis. Gut 2011, 60:1379–1388 [PubMed: 21471572]

28. Zhan X, Wan J, Zhang G, Song L, Gui F, Zhang Y, Li Y, Guo J, Dawra RK, Saluja AK, Haddock AN, Zhang L, Bi Y, Ji B. Elevated intracellular trypsin exacerbates acute pancreatitis and chronic pancreatitis in mice. Am J Physiol Gastrointest Liver Physiol 2019, 316:G816–G825 [PubMed: 30943050]

29. Huang H, Swidnicka-Siergiejko AK, Daniluk J, Gaiser S, Yao Y, Peng L, Zhang Y, Liu Y, Dong M, Zhan X, Wang H, Bi Y, Li Z, Ji B, Logsdon CD. Transgenic expression of PRSS1 R122H sensitizes mice to pancreatitis. Gastroenterology 2019 8 13 [Epub ahead of print]

30. Gui F, Zhang Y, Wan J, Zhan X, Yao Y, Li Y, Haddock AN, Shi J, Guo J, Chen J, Zhu X, Edenfield BH, Zhuang L, Hu C, Wang Y, Mukhopadhyay D, Radisky ES, Zhang L, Lugea A, Pandol SJ, Bi Y, Ji B. Trypsin activity governs increased susceptibility to pancreatitis in mice expressing human PRSS1 R122H. J Clin Invest 2019 9 24 [Epub ahead of print]

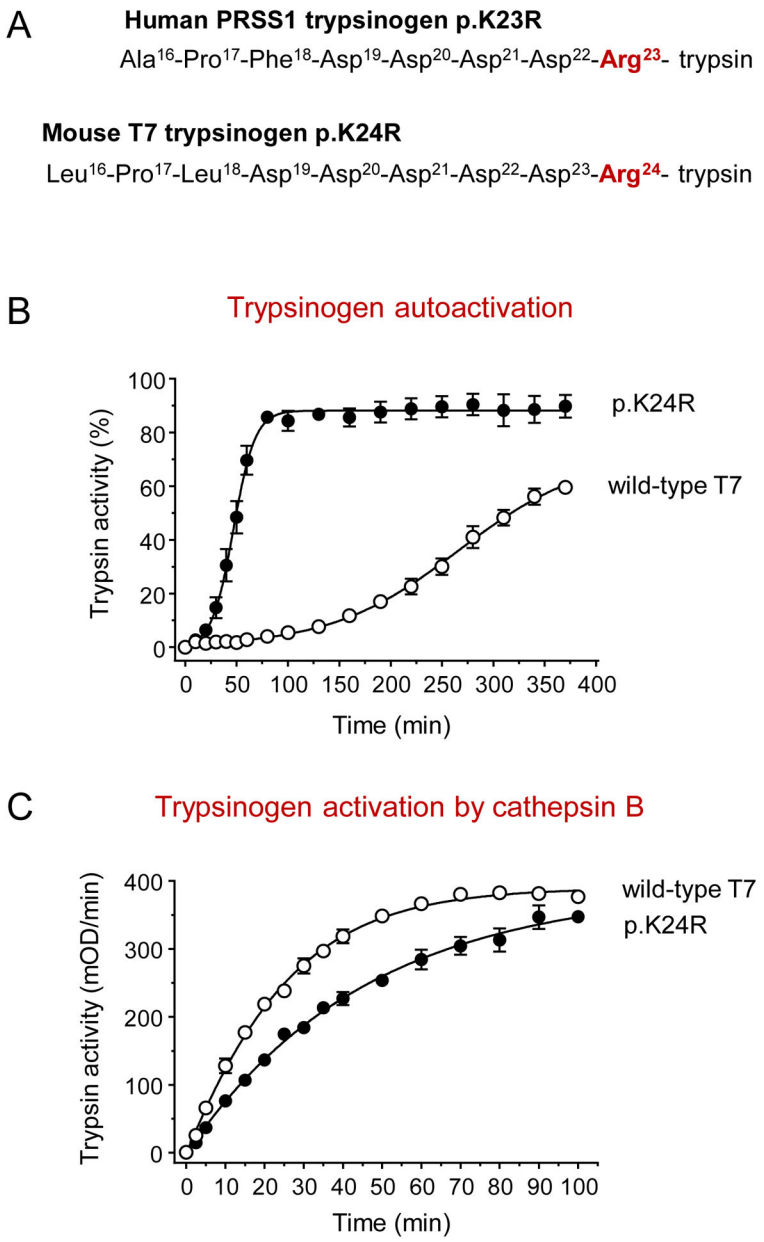

Figure 1.

Effect of mutation p.K24R on the activation of mouse cationic trypsinogen (isoform T7). (**A**) The activation peptide sequences of human (PRSS1) and mouse (T7) cationic trypsinogen. Position of analogous mutations p.K23R and p.K24R are highlighted in red. (**B**) Autoactivation of purified wild-type (empty circles) and p.K24R mutant (solid circles) T7 trypsinogen. Data points represent mean ± standard deviation (n = 3). (**C**) Activation of purified wild-type and p.K24R mutant T7 trypsinogen by cathepsin B. See Methods for experimental details. Data points represent mean ± standard deviation (n = 3).

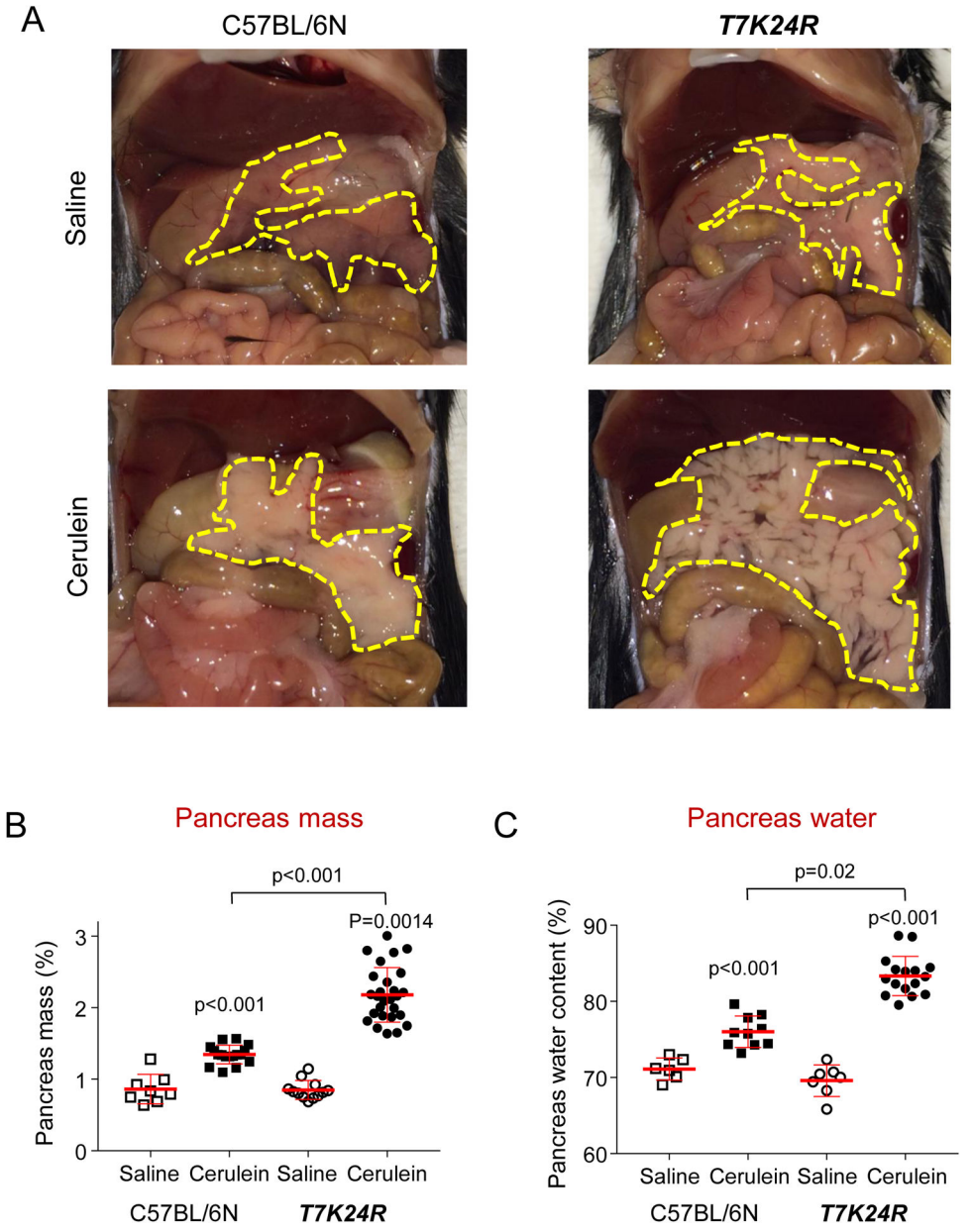

Figure 2.

Cerulein-induced acute pancreatitis in *T7K24R* mice. (**A**) Representative pictures of the pancreas of C57BL/6N and *T7K24R* mice given 12 hourly injections of saline or cerulein. (**B**) Pancreas mass of C57BL/6N and *T7K24R* mice given saline or cerulein, expressed as percent of body mass. (**C**) Pancreatic water content of *T7K24R* and C57BL/6N mice treated with saline or cerulein, expressed as percent wet pancreas weight. Individual data points with mean (horizontal bar) and standard deviation are shown. See Methods for experimental details.

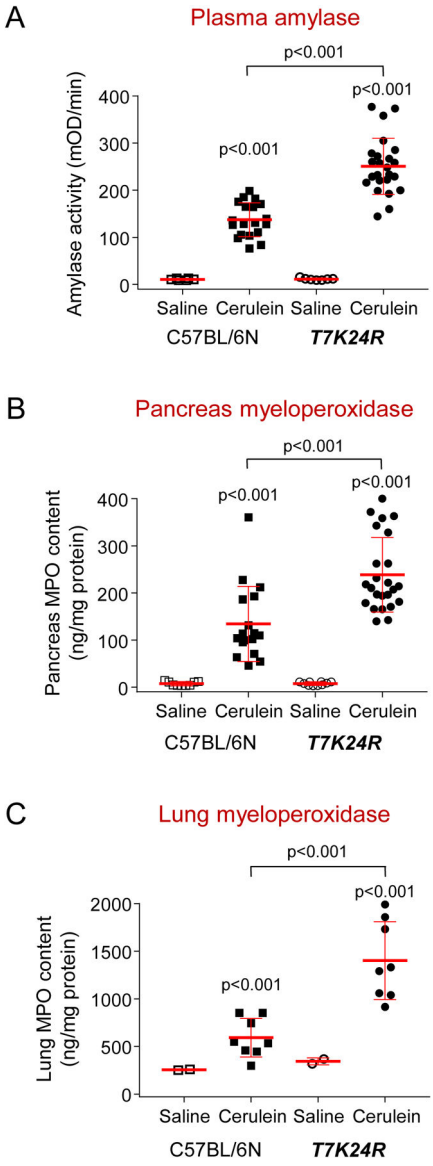

Figure 3.

Cerulein-induced acute pancreatitis in *T7K24R* mice. (**A**) Plasma amylase activity in C57BL/6N and *T7K24R* and mice given 12 hourly injections of saline or cerulein. (**B**) Pancreatic myeloperoxidase (MPO) content of C57BL/6N and *T7K24R* mice treated with saline or cerulein. (**C**) Lung MPO content of C57BL/6N and *T7K24R* mice treated with saline or cerulein. Individual data points with mean (horizontal bar) and standard deviation are shown. See Methods for experimental details.

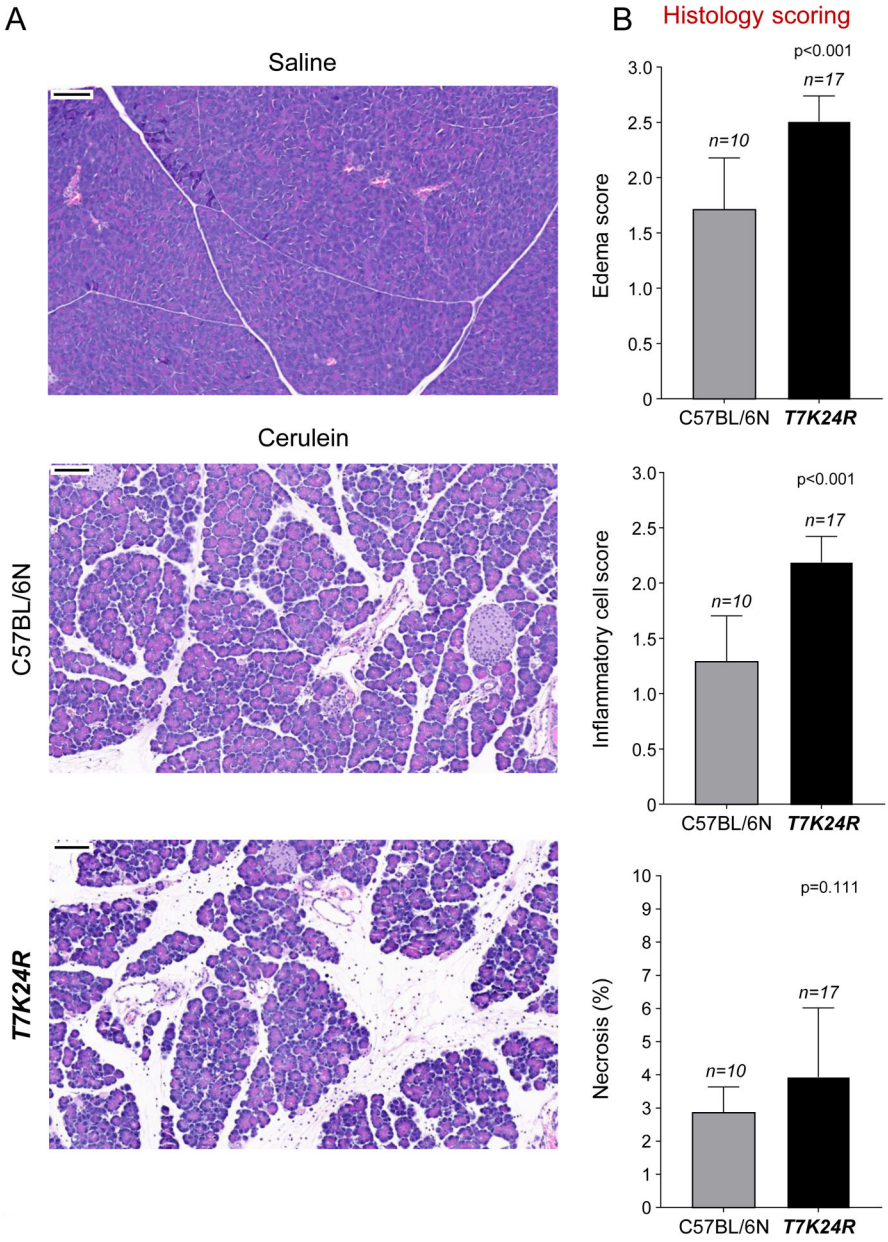

Figure 4.

Histology of cerulein-induced acute pancreatitis in *T7K24R* mice. (**A**) Representative hematoxylin-eosin stained histological sections of the pancreas from saline and cerulein-treated mice. Scale bars correspond to 100 μm. (**B**) Histology scoring for edema, inflammatory cell infiltration, and acinar cell necrosis in cerulein-treated mice. Mean values with standard deviation are shown. See Methods for details.

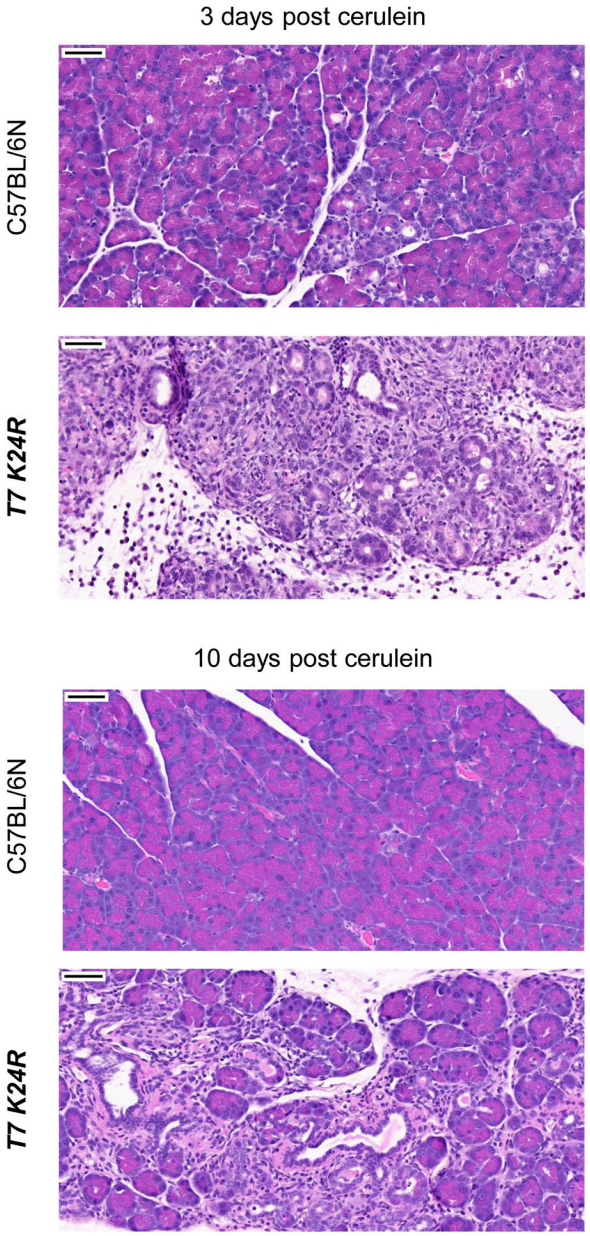

Figure 5.

Histology of pancreatitis induced by sustained cerulein stimulation in *T7K24R* mice. Mice were treated with saline or cerulein for 2 days (8 hourly injections per day) and sacrificed 3 days or 10 days after the last injection. Representative hematoxylin-eosin stained histological sections of the pancreas from cerulein-treated mice are shown. The pancreas of mice given saline was normal (not shown). Scale bars correspond to 50 μm.

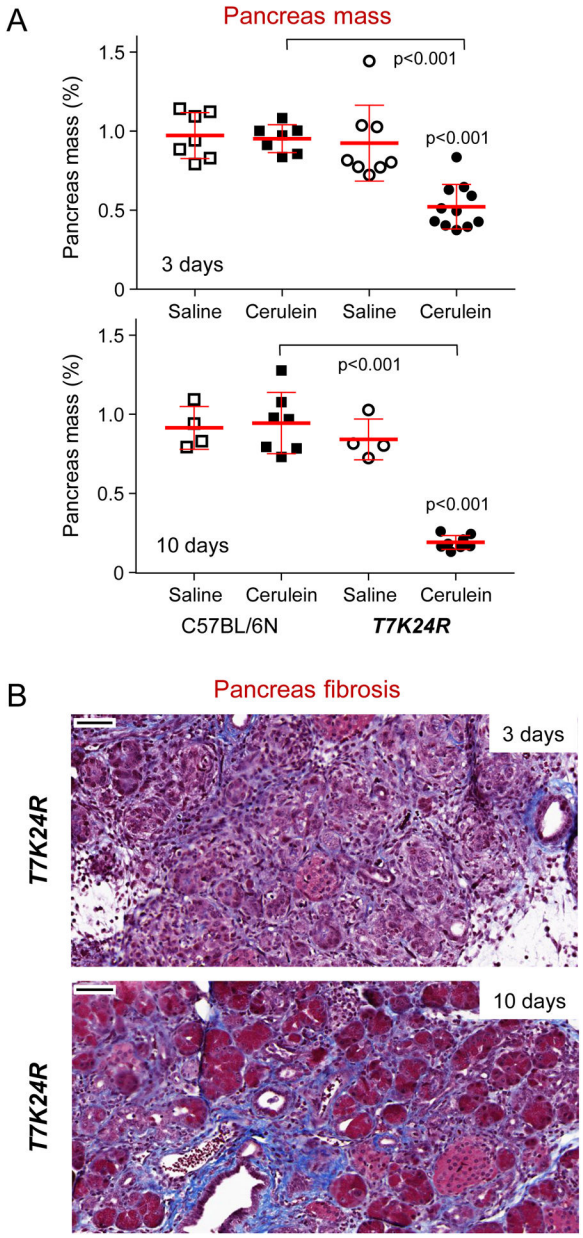

Figure 6.

Pancreas mass and pancreas fibrosis after sustained cerulein stimulation in *T7K24R* mice. Mice were treated with saline or cerulein for 2 days (8 hourly injections per day) and sacrificed 3 days or 10 days after the last injection. (**A**) Pancreas mass (as percent of body mass) of C57BL/6N and *T7K24R* mice given saline or cerulein. Individual data points with mean (horizontal bar) and standard deviation are shown. (**B**) Masson's trichrome staining of pancreas sections from cerulein-treated *T7K24R* mice 3 days and 10 days after the last injection. Blue color indicates fibrosis. Scale bars correspond to 50 μm.

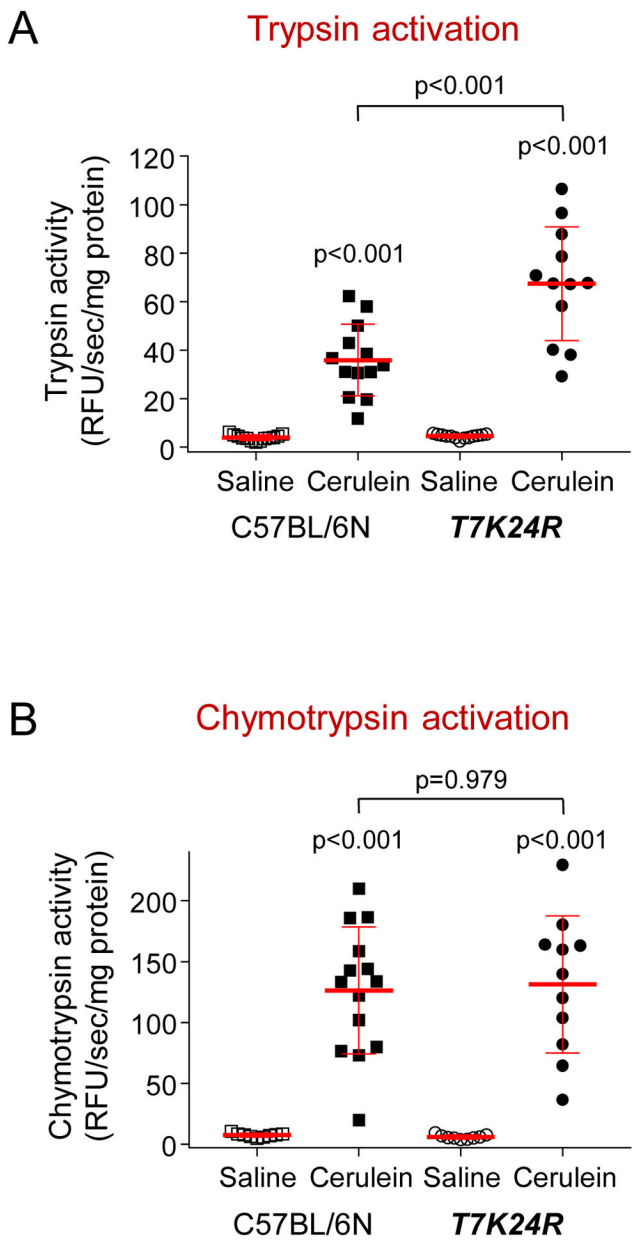

Figure 7.

Intrapancreatic protease activation in *T7K24R* mice. Trypsin (**A**) and chymotrypsin (**B**) activities were measured 30 minutes after a single saline or cerulein injection. Individual data points with mean (horizontal bar) and standard deviation are shown. See Methods for experimental details.